

# LeAdQA: LLM-Driven Context-Aware Temporal Grounding for Video Question Answering

Xinxin Dong<sup>1</sup>, Baoyun Peng<sup>2\*</sup>, Haokai Ma<sup>3</sup>,  
Yufei Wang<sup>1</sup>, Zixuan Dong<sup>1</sup>, Fei Hu<sup>1</sup>, Xiaodong Wang<sup>1</sup>,

<sup>1</sup>National Key Laboratory of Parallel and Distributed Computing, College of Computer Science and Technology,  
National University of Defense Technology

<sup>2</sup>Academy of Military Sciences

<sup>3</sup>National University of Singapore  
pengbaoyun13@alumni.nudt.edu.cn

## Abstract

Video Question Answering (VideoQA) requires identifying critical moments in long videos and reasoning about their causal relationships to answer semantically complex questions. Current approaches suffer from two key limitations: (1) task-agnostic sampling that overwhelms relevant content with irrelevance, and (2) heuristic retrieval that captures superficial patterns while missing causal-temporal structures essential for complex reasoning. To tackle these limitations, we propose LeAdQA, a novel approach that combines causal-aware query refinement with fine-grained visual grounding. Our method leverages LLMs to reformulate question-option pairs, resolving causal ambiguities and sharpening temporal focus. These refined queries guide precise retrieval of salient segments, while an adaptive fusion mechanism integrates evidence to maximize relevance. Finally, an MLLM processes the integrated visual-textual cues to generate contextually-grounded answers. LeAdQA achieves state-of-the-art performance on the NEX-T-QA, IntentQA, and NEX-T-GQA datasets, demonstrating that precise visual clues significantly enhances the model’s reasoning on complex questions while maintaining computational efficiency.

## Introduction

Video understanding is increasingly critical across diverse domains, spanning educational platforms, entertainment systems, surveillance networks, and autonomous vehicles (Wang et al. 2024c; Maaz et al. 2023). Within this landscape, Video Question Answering (VideoQA) emerges as a foundational capability that requires models to comprehend complex spatio-temporal dynamics and reason about visual content in response to queries in natural language (Xiao et al. 2021; Li et al. 2023b). However, transitioning from short-form to long-form video analysis introduces unprecedented challenges that reshape the problem space. Extended video sequences exhibit a sparse distribution of critical information within redundant content, posing two core technical challenges: (1) identifying and extracting relevant visual cues across temporally distant segments; (2) maintaining fine-grained temporal resolution while processing computationally intensive long sequences.

\*Corresponding Author.

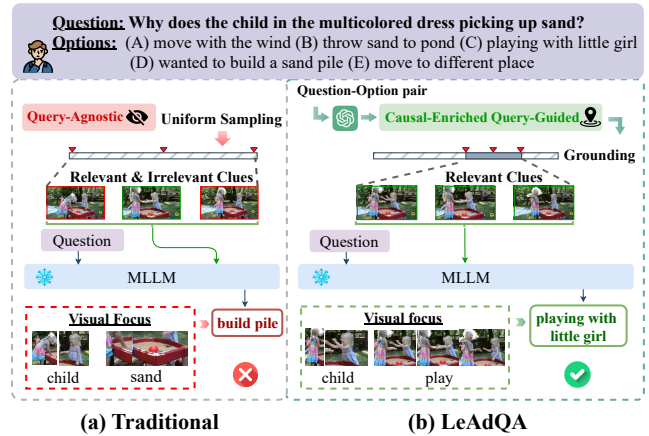


Figure 1: Architecture comparison: (a) Traditional frameworks incorporate irrelevant spatiotemporal data, hindering visual reasoning; (b) LeAdQA enables precision localization of query-relevant moments via temporal grounding.

Early VideoQA methods relied on 3D convolutional networks (Tran et al. 2015), hierarchical modeling (Lu et al. 2016), and attention-based frame localization (Ren et al. 2016) to capture spatiotemporal patterns. However, these approaches primarily focused on surface-level correlations and lacked the semantic abstraction required for complex reasoning (Lei et al. 2018). The emergence of Multimodal Large Language Models (MLLMs) has revolutionized video understanding (Liu et al. 2024; Wang et al. 2024a). Current MLLM-based approaches fall into three paradigms: end-to-end methods processing visual and textual tokens jointly (Wang et al. 2024a; Maaz et al. 2023), two-stage approaches separating visual understanding from linguistic reasoning (Zhang et al. 2023; Yu et al. 2024), and hybrid frameworks combining both strategies (Wang et al. 2024c; Li et al. 2023b). These MLLM-based methods have achieved remarkable progress in video question answering by leveraging the inherent reasoning capabilities of large language models (LLMs) to bridge the semantic gap between visual content and natural language queries, enabling more sophisticated inference beyond traditional pat-

tern matching approaches.

Despite these advances, current VideoQA methods remain constrained in long-form understanding due to several limitations. Foremost, the neglect of causal relationships between questions and candidate answers leads to treating options as isolated entities (Wei et al. 2023; Zang et al. 2023)—overlooking semantic interdependencies that could enable comparative reasoning critical for multiple-choice scenarios. Such cognitive gap propagates to visual processing, where coarse temporal grounding induces fragmented localization (Guo et al. 2024; Wu et al. 2025): critical moments splinter into misaligned segments that fracture causal chains (e.g., separating triggers from consequences). Compounding these errors, the inherent redundancy of long videos forces models into a lose-lose computational bind (Wang et al. 2024b)—where global processing may drown signals in noise, while aggressive sampling discards sparse pivotal events.

To address these challenges, we present **LeAdQA**, a novel LLM-Driven Context-Aware Temporal Grounding framework that enhances MLLMs for VideoQA through integrated causal-temporal reasoning. Our approach operates through three key innovations: First, LeAdQA leverages LLMs to reformulate question-option (Q-O) pairs, explicitly injecting causal relationships to resolve linguistic ambiguities and establishing "leading" contextual cues for reasoning. Second, unlike traditional frameworks that incorporate irrelevant spatiotemporal data, LeAdQA enables precision localization of query-relevant moments through dedicated temporal grounding, as illustrated in Figure 1. These causally-enhanced queries drive a cross-modal transformer that dynamically localizes critical video segments by aligning textual semantics with visual content, significantly outperforming question-only localization methods. Third, we introduce an adaptive interval fusion mechanism that evaluates candidate segments using dual criteria: temporal overlap (IoU) and salience scores. This filtering approach preserves semantically coherent intervals while eliminating noise, enabling MLLMs to effectively model Q-O causality alongside visual features for precise temporal reasoning in long-form VideoQA.

Extensive experiments on NExT-QA (Xiao et al. 2021), IntentQA (Li et al. 2023b), and NExT-GQA (Xiao et al. 2024) demonstrate consistent improvements over state-of-the-art (SOTA) approaches. Our empirical analysis reveals that LLM-mediated causal resolution enhances temporal grounding precision, with higher tIoU strongly correlating with QA accuracy, confirming that informational quality is more critical than quantity. Our main contributions include:

- We present LeAdQA, a novel LLM-driven architecture that addresses causal-temporal gaps through: rewriting question-option pairs to inject causal dependencies, leveraging option semantics as cross-modal constraints, and generating refined temporal proposals via context-aware grounding.
- We propose an **adaptive NMS module** that combines temporal overlap with LLM-extracted causal relevance scores, preserving coherent segments while eliminating

redundancy.

- Comprehensive evaluation across three datasets demonstrates significant improvements in temporal localization and QA accuracy.

## Related Works

### Video Temporal Grounding

Video Temporal Grounding (VTG) localizes moments in untrimmed videos that semantically align with textual queries. Current approaches follow two paradigms: two-stage and end-to-end methods. Two-stage approaches generate temporal proposals (Gao et al. 2017; Xu et al. 2018) then perform cross-modal matching, but suffer from computational inefficiency due to dense candidate sampling. End-to-end methods directly regress temporal boundaries, with transformer-based approaches like MomentDETR (Lei, Berg, and Bansal 2021) and QD-DETR (Moon et al. 2023) formulating VTG as set prediction with enhanced cross-attention. Despite efficiency gains, current methods still struggle with long-range dependencies and precise alignment. Unlike VTG’s descriptive event-boundary queries, VideoQA grounding requires multimodal reasoning for discriminative answer selection.

### Multimodal Large Language Models

The success of large language models (LLMs) in natural language processing has sparked increasing interest in extending their capabilities to multimodal tasks (Radford et al. 2021; Liu et al. 2024). One line of research translates non-textual inputs into natural language to align visual and textual modalities. For instance, OFA (Wang et al. 2022a) performs visual-to-text translation while LaViLa (Zhao et al. 2023) generates video captions. Alternatively, some approaches employ trainable interface layers for direct modality bridging. Flamingo (Alayrac et al. 2022) links CLIP (Radford et al. 2021) vision encoders to LLMs via learned projections, while BLIP-2 (Li et al. 2023a) and LLaVA (Liu et al. 2024) further refine alignment using Q-Former and MLP-based adapters, respectively. Recent video-oriented models such as Video-ChatGPT (Maaz et al. 2023) incorporate temporal dynamics to support video-language understanding. Although effective, these methods often rely on intensive cross-modal training and incur significant computational overhead.

### Video Question Answering

VideoQA aims to answer questions based on video content and textual queries, posing challenges in spatiotemporal reasoning and cross-modal alignment. Early approaches adopted cross-attention mechanisms (Chu et al. 2018) for visual-textual alignment. Subsequent work explores memory networks (Yu et al. 2020) for multi-hop reasoning and graph neural networks (Seo et al. 2021) to model object-scene interactions. More recent advances leverage pre-trained vision-language models and LLMs, with strategies such as fine-tuning (Tan et al. 2024), constructing spatial-temporal scene graphs (Fei et al. 2024), and filtering captions without additional training (Zhang et al. 2023; Islam

et al. 2024). VideoAgent (Wang et al. 2025) further employs LLMs as iterative information extractors. While effective, many of these methods underutilize fine-grained visual cues. In contrast, our framework can better capture detailed visual semantics to improve complex reasoning.

## Method

We present **LeAdQA**, a novel VideoQA framework that integrates causal-aware language modeling and temporal grounding to enhance MLLMs in contextual understanding and answer reasoning. As illustrated in Figure 2, LeAdQA comprises three core components: (1) LLM-guided question-option rephrasing, (2) motion-aware temporal grounding, and (3) multi-threshold interval fusion for robust localization.

### Problem Formulation

Given a video  $\mathcal{V}$  and a multiple-choice question  $Q$  with answer candidates  $\mathcal{O} = \{o_i\}_{i=1}^N$ , where  $N$  is the number of candidate options, we define  $q_i = (Q, o_i)$  as the query corresponding to option  $o_i$ . LeAdQA aims to (i) generate semantically enriched query descriptions  $\{q'_i\}_{i=1}^N$  using an LLM, (ii) localize temporally grounded video segments that support or contradict each  $q'_i$ , and (iii) aggregate temporal evidence for answer prediction.

### LLM-Driven Question-Option Rephrase

To enhance causal reasoning and video alignment, each query  $q'_i$  is rephrased using an LLM  $\mathcal{M}_r$  with a structured prompt  $\mathcal{P}_r$ :

$$q'_i = \mathcal{M}_r(\mathcal{P}_r(Q, o_i)). \quad (1)$$

The output  $q'_i$  describes a hypothetical video situation under which option  $o_i$  is true, making implicit causal cues explicit. The full set of enriched queries is denoted as  $\mathcal{Q}' = \{q'_i\}_{i=1}^N$ .

### Motion-Aware Temporal Grounding

**Unified Formulation.** Following the unified spatiotemporal alignment framework (Lin et al. 2023), we divide video  $\mathcal{V}$  into a sequence of overlapping clips  $\{v_j\}_{j=1}^{L_v}$  of fixed duration  $l$ , centered at timestamps  $t_j$ . For each clip  $v_j$  and query  $q'_i$ , the model predicts:

- **Foreground Flag:**  $f_{ij} \in \{0, 1\}$ : Indicates whether  $v_j$  is relevant to query  $q'_i$ .
- **Boundary Offset:**  $\delta_{ij} = [\delta_{ij}^s, \delta_{ij}^e]$ : Denotes the temporal offset from  $t_j$  to the predicted segment boundaries.
- **Saliency Score:**  $s_{ij} \in [0, 1]$ : Measures semantic relevance between  $v_j$  and query  $q'_i$ .

The resulting grounded segment is:

$$b_{ij} = [t_j - \delta_{ij}^s, t_j + \delta_{ij}^e], \quad (2)$$

and the set of relevant segments for query  $q'_i$  is  $\mathcal{B}_i = \{b_{ij} \mid f_{ij} = 1 \wedge s_{ij} > \tau_p\}$ . Here,  $\tau_p \in [0, 1]$  is a saliency threshold that filters out low-relevance segments. It is tuned on a validation set and held fixed during inference.

**Architecture and Training** We encode an enriched query  $q'_i$  with  $L_q$  tokens and a video  $\mathcal{V}$  with  $L_v$  clips separately using text and video encoders, followed by FFNs to project features into a shared  $d$ -dimensional space, obtaining token-level features  $\mathbf{F}_t$  and clip-level features  $\mathbf{F}_v$  respectively:

$$\mathbf{F}_t = \{q'_{i',j}\}_{j=1}^{L_q} \in \mathbb{R}^{L_q \times d} \quad (3)$$

$$\mathbf{F}_v = \{v_j\}_{j=1}^{L_v} \in \mathbb{R}^{L_v \times d} \quad (4)$$

**Cross-Modal Fusion.** We apply modality and positional embeddings to get  $\tilde{\mathbf{F}}_v$  and  $\tilde{\mathbf{F}}_t$ , concatenate them into  $\mathbf{F}_z = [\tilde{\mathbf{F}}_v; \tilde{\mathbf{F}}_t]$ , and are processed by  $K_t$  Transformer layers before being passed to the subsequent prediction head:

$$\mathbf{F}_z^{(l)} = \text{MLP}(\text{MSA}(\mathbf{F}_z^{(l-1)})), \quad l = 1, \dots, K_t. \quad (5)$$

**Prediction Heads and Losses.** We employ three prediction heads to optimize distinct grounding objectives:

- **Foreground Head:** This head predicts the binary label  $\hat{f}_{ij}$  for each clip  $v_j$  using a stack of  $1 \times 3$  convolutional layers with ReLU activation. The training objective is binary cross-entropy:

$$\mathcal{L}_{fg} = - \sum_{j=1}^{L_v} [f_{ij} \log \hat{f}_{ij} + (1 - f_{ij}) \log(1 - \hat{f}_{ij})] \quad (6)$$

- **Boundary Head:** This head predicts the segment boundaries  $\hat{\delta}_{ij}^s$  and  $\hat{\delta}_{ij}^e$  for each foreground clip. The loss combines Smooth- $L_1$  distance between predicted and ground-truth offsets, and an IoU-based loss between predicted segment  $\hat{b}_{ij}$  and ground-truth  $b_{ij}$ :

$$\mathcal{L}_{reg} = \mathbb{1}_{\{f_{ij}=1\}} [\lambda_{L1} \mathcal{L}_{smooth} + \lambda_{IoU} \mathcal{L}_{IoU}] \quad (7)$$

- **Saliency Head:** This head computes the cosine similarity between visual and textual embeddings to assign a saliency score  $\hat{s}_{ij}$ . We incorporate both intra-video and inter-video contrastive learning to encourage fine-grained and global discriminability:

$$\mathcal{L}_{sal} = \lambda_{inter} \mathcal{L}_{sal}^{inter} + \lambda_{intra} \mathcal{L}_{sal}^{intra} \quad (8)$$

The total loss over all clips and all query-option pairs is:

$$\mathcal{L}_{total} = \frac{1}{N} \sum_{i=1}^N \sum_{j=1}^{L_v} (\mathcal{L}_{fg} + \mathcal{L}_{reg} + \mathcal{L}_{sal}) \quad (9)$$

### Multi-Threshold Interval Fusion

After grounding, we obtain  $K_s$  top-ranked segments for each query  $q'_i$ , resulting in the candidate set  $\mathcal{C} = \{c_k = [t_k^s, t_k^e]\}_{k=1}^{N \times K_s}$ . These segments represent the model's predicted intervals, with  $t_k^s$  and  $t_k^e$  denoting the start and end timestamps, respectively. The segments are then refined through merging and fusion to reduce redundancy and enhance temporal grounding.

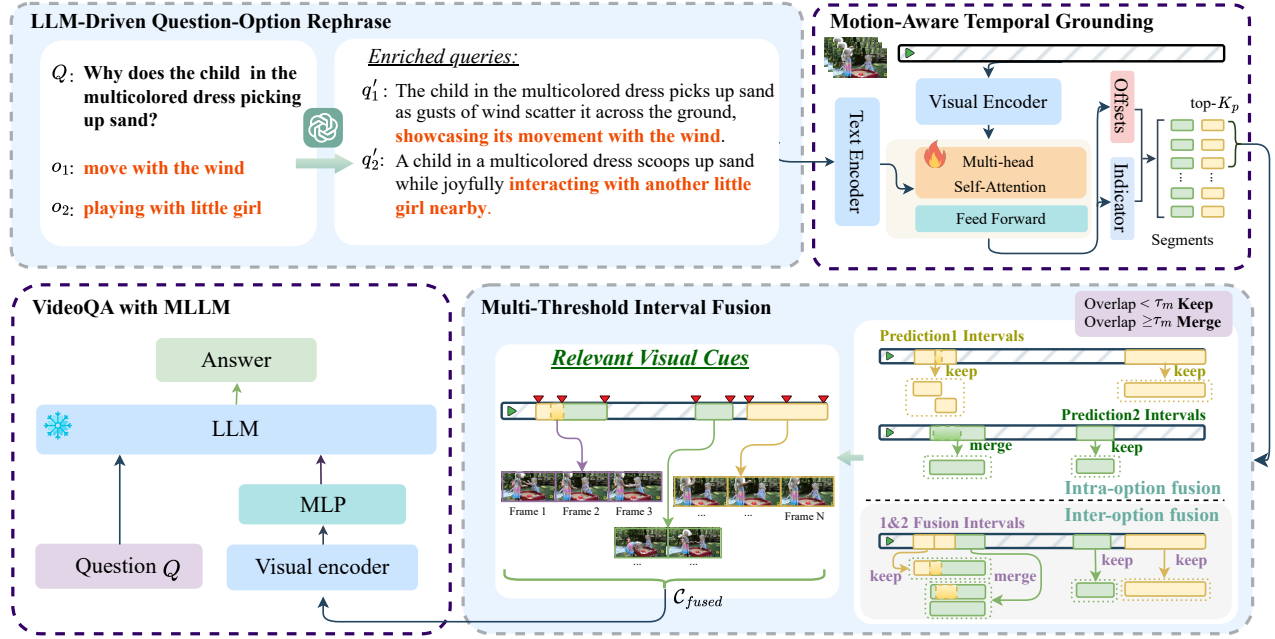


Figure 2: The architecture of LeAdQA. Question-option pairs are first rephrased by LLMs to generate enhanced descriptions, which are then used to localize relevant visual segments. Temporal intervals are subsequently filtered and merged through overlap threshold analysis. Finally, the optimized segments are fed into an MLLM to generate the final answer.

**IoU-Based Merging.** Two temporal intervals  $c_k$  and  $c_{k'}$  are merged if their Intersection over Union (IoU) exceeds a predefined threshold  $\tau_m$ :

$$\text{IoU}(c_k, c_{k'}) = \frac{\text{overlap}}{\text{union}} \geq \tau_m \quad (10)$$

where:

$$\text{overlap} = \max(0, \min(t_k^e, t_{k'}^e) - \max(t_k^s, t_{k'}^s)) \quad (11)$$

$$\text{union} = (t_k^e - t_k^s) + (t_{k'}^e - t_{k'}^s) - \text{overlap} \quad (12)$$

If IoU exceeds  $\tau_m$ , the intervals are merged:

$$\text{Merge}(c_k, c_{k'}) = [\min(t_k^s, t_{k'}^s), \max(t_k^e, t_{k'}^e)]. \quad (13)$$

This approach reduces temporal redundancy by retaining only the most relevant intervals.

**Hierarchical Fusion Strategy.** We employ a two-stage hierarchical fusion process to integrate temporal evidence:

- **Intra-option fusion:** Consolidates overlapping temporal intervals within each enriched query to eliminate redundant segments and create coherent evidence units.
- **Inter-option fusion:** Aggregates the consolidated intervals across different answer options to capture contextual information and enable comparative reasoning.

These fusion steps help to maintain a diverse and non-redundant set of segments, improving the accuracy of temporal grounding.

During inference, all prediction heads contribute, and NMS is applied to remove redundant intervals based on high overlap. The final non-redundant segments,  $\mathcal{C}_{\text{fused}}$ , are used for answer selection, ensuring that the most relevant video segments are chosen to answer the query.

## Video Question Answering with MLLMs

To perform answer prediction, we employ MLLMs that integrates temporally grounded visual segments and textual queries. Building upon the video-language framework of (Wang et al. 2024a; Bai et al. 2025), we construct a multimodal input consisting of the original video  $\mathcal{V}$ , the natural language question  $Q$ , and the fused temporal segments  $\mathcal{C}_{\text{fused}}$  produced by our grounding module.

To extract representative visual context, we uniformly sample  $K_f$  keyframes  $\{e_k\}_{k=1}^{K_f}$  from  $\mathcal{C}_{\text{fused}}$ . Each frame  $e_k$  is encoded using the CLIP-ViT (Radford et al. 2021) visual encoder to obtain patch-level embeddings:

$$\mathbf{E}_v = \text{CLIP-ViT}(\{e_k\}_{k=1}^{K_f}) \in \mathbb{R}^{K_f \times N_p \times d_v}, \quad (14)$$

where  $N_p$  is the number of patches per frame, and  $d_v$  denotes the visual embedding dimension.

These features are projected to match the LLM input space via a trainable MLP:

$$\mathbf{H}_v = \text{MLP}(\mathbf{E}_v) \in \mathbb{R}^{K_f \times N_p \times d_h} \quad (15)$$

where  $d_h$  denotes the hidden dimension required by the language model.

To form the multimodal input, the flattened visual tokens  $\mathbf{H}_v^{\text{flat}}$  are concatenated with the embedded textual prompt derived from  $Q$  and the candidate options  $\mathcal{O} = \{o_i\}_{i=1}^N$  using the answering prompt template  $\mathcal{P}_a(Q, \mathcal{O})$ :

$$\mathbf{E}_p = \text{Embed}(\mathcal{P}_a(Q, \mathcal{O})) \quad (16)$$

$$\mathcal{A}_p = \mathcal{M}_a(\text{concat}[\mathbf{W}_p \mathbf{H}_v^{\text{flat}}, \mathbf{E}_p]) \quad (17)$$

Methods	Answering			Grounding				
	Acc@QA	Acc@GQA	mIoP	IoP@0.3	IoP@0.5	mIoU	IoU@0.3	IoU@0.5
Human	93.3	82.1	72.1	91.7	86.2	61.2	86.9	70.3
Random	20.0	1.7	21.1	20.6	8.7	21.1	20.6	8.7
IGV (Li et al. 2022)	50.1	10.2	21.4	26.9	18.9	14.0	19.8	9.6
VGt (Xiao et al. 2024)	50.9	12.7	24.7	26.0	24.6	3.0	4.2	1.4
VIOLETv2 (Fu et al. 2023)	52.9	12.8	23.6	25.1	23.3	3.0	4.3	1.3
Temp [Swin] (Xiao et al. 2024)	55.9	14.4	25.3	26.4	25.3	3.0	3.6	1.7
Temp [CLIP] (Xiao et al. 2024)	59.4	14.7	24.1	26.2	24.1	6.8	8.3	3.7
Temp [CLIP] (NG+) (Xiao et al. 2024)	60.2	16.0	25.7	31.4	25.5	12.1	17.5	8.9
FrozenBiLM (Yang et al. 2022)	69.1	15.8	22.7	25.8	22.1	7.1	10.0	4.4
FrozenBiLM (NG+) (Xiao et al. 2024)	<u>70.8</u>	17.5	24.2	28.5	23.7	9.6	13.5	6.1
SeViLA (Yu et al. 2024)	68.1	16.6	<u>29.5</u>	<u>34.7</u>	22.9	<b>21.7</b>	<u>29.2</u>	<u>13.8</u>
QGAC-TR (Xu et al. 2024)	63.6	<u>18.3</u>	28.3	32.8	<u>27.7</u>	15.7	18.6	11.7
<b>LeAdQA-7B</b>	67.5	19.2	<b>30.3</b>	<b>39.6</b>	<b>29.5</b>	<u>20.5</u>	<b>31.3</b>	<b>17.5</b>
<b>LeAdQA-34B</b>	<b>77.0</b>	<b>20.7</b>						

Table 1: Performance on NExT-GQA test set. Answering and Grounding are the metrics designed to evaluate performance in VideoQA and grounded QA, respectively. Other results are taken from (Xu et al. 2024).

where  $\mathcal{M}_a$  denotes the MLLM,  $\mathbf{W}_p$  is a learnable projection matrix aligning visual features with language embeddings, and the final answer is  $\mathcal{A}_p$ .

$\mathcal{A}_p$  is generated in free-form text, conditioned on both the temporally grounded visual content and the structured textual prompt. Notably,  $\mathcal{P}_a$  differs from the earlier rewriting prompt  $\mathcal{P}_r$  used for generating the semantically enriched queries while  $\mathcal{P}_r$  is designed to enhance temporal grounding through causal enrichment,  $\mathcal{P}_a$  is tailored for answer decoding and decision making based on the fused multimodal evidence.

This final stage enables LeAdQA to jointly reason over visual content and query semantics, completing the VideoQA pipeline with grounded, context-aware answer generation.

## Experiments

### Experimental Settings

**Datasets.** Our evaluation utilizes three established video question answering datasets that collectively assess diverse reasoning capabilities:

**NExT-QA** (Xiao et al. 2021) is a comprehensive benchmark featuring 5,440 videos (average 44 seconds) with 47,692 multiple-choice questions. Questions are categorized into three reasoning types: temporal action localization (Tem.), causal inference (Cau.), and descriptive analysis (Des.), each with five answer options.

**IntenQA** (Li et al. 2023b) focuses on context-aware video intent reasoning with 4,303 videos and 16,297 questions categorized into: Causal Why (CW), Causal How (CH), and temporal action localization (Tem.).

**NExT-GQA** (Xiao et al. 2024) extends NExT-QA by providing visual evidence annotations. It contains 5,417 videos, with 1,557 videos having 10,531 precisely annotated temporal segments corresponding to 8,911 question-answer pairs focused on temporal (Tem.) and causal (Cau.) reasoning.

**Evaluation Metrics.** For VideoQA, we use accuracy as the main metric. For temporal grounding, we adopt Intersection over Prediction (IoP) (Xiao et al. 2024) and temporal IoU (tIoU) to assess segment containment and overlap with ground truth, reporting both mean scores and hit rates at 0.3 and 0.5 thresholds. We also illustrate Grounded QA Accuracy (Acc@GQA), which considers a prediction correct only if it answers correctly and its temporal segment achieves an  $\text{IoP} \geq 0.5$ . This reflects a model’s ability to combine semantic understanding with accurate temporal localization.

**Implementation Details.** Our framework integrates causal reasoning, multimodal alignment, and efficient inference to enable comprehensive video understanding. We first employ GPT-4o (Achiam et al. 2023) to enhance question-option pairs by inferring implicit causal relationships via constrained text generation. We adopt UniVTG (Lin et al. 2023) as our grounding model, which consists of 4 Transformer encoder layers. Each layer is configured with 1024 hidden dimensions and 8 attention heads, along with specialized output heads for downstream prediction. Each question is equipped with five descriptions and we select top-k ( $k \in \{1, 3, 5\}$ ) predicted intervals. Multiple overlap thresholds  $[0.1, 0.3, 0.5, 0.7, 0.9]$  guide interval retention or merging decisions based on temporal alignment, enabling visual cue integration. Our final answer generation leverages Tarsier-7B, Tarsier-34B (Wang et al. 2024a) and Qwen2.5-VL-3B-Instruct and Qwen2.5-VL-7B-Instruct (Bai et al. 2025) models with uniform, interval-focused, and hybrid sampling strategies. We evaluate performance across  $[1, 2, 4, 8, 16, 32, 48]$  frames to balance accuracy and efficiency. We do our experiments on four A100 40G GPUs.

## Results and Analysis

**Baselines.** We evaluate LeAdQA on the test sets of **NExT-GQA** and **IntentQA**, with the validation set of **NExT-QA**.

For **NExT-GQA**, we evaluate both multi-choice video QA and temporal grounding tasks, comparing LeAdQA against baselines including IGV (Li et al. 2022), VGT (Xiao et al. 2024), VIOLETv2 (Fu et al. 2023), Temp[Swin], Temp[CLIP], Temp[CLIP(NG+)] (Xiao et al. 2024), Frozen-BiLM (Yang et al. 2022), FrozenBiLM (NG+) (Xiao et al. 2024), SeViLA (Yu et al. 2024), QGAC-TR (Xu et al. 2024). We further evaluate Tarsier-7B and Tarsier-34B (Wang et al. 2024a), as well as Qwen2.5VL-3B and Qwen2.5VL-7B (Bai et al. 2025), both with and without LeAdQA integration.

For **NExT-QA**, comparisons include video QA methods such as video transformers like InternVideo (Wang et al. 2022b), open-source LLM-based approaches including SeViLA and MVU (Ranasinghe et al. 2024), alongside proprietary LLM-driven models like LLoVi (Zhang et al. 2023), VideoAgent (Wang et al. 2025), MoReVQA (Min et al. 2024), IG-VLM (Kim et al. 2024), LangRepo (Kahatapitiya et al. 2024), LVNet (Park et al. 2024), and VideoTree (Wang et al. 2024c). We also assess Tarsier-7B and Tarsier-34B with and without LeAdQA integration.

For **IntentQA**, we compare LeAdQA with SeViLA, LLoVi, LangRepo, LVNet, and Tarsier models, both standalone and integrated with LeAdQA.

**Comparison with Baselines.** Table 1 presents temporal grounding performance on NExT-GQA, while Tables 2, 3, and 4 report VideoQA accuracy on NExT-GQA, NExT-QA, and IntentQA, respectively.

Model	Tem.	Cau.	Avg.
Qwen-3B	57.4	51.4	53.9
<b>LeAdQA-3B'</b>	59.8 (+2.4)	52.8 (+1.4)	55.7 (+1.8)
Qwen-7B	64.4	67.3	66.1
<b>LeAdQA-7B'</b>	65.6 (+1.1)	69.1 (+1.8)	67.7 (+1.6)
Tarsier-7B	62.1	67.9	65.5
<b>LeAdQA-7B</b>	63.6 (+1.5)	70.4 (+2.5)	67.5 (+2.0)
Tarsier-34B	<u>71.7</u>	<u>77.7</u>	<u>75.2</u>
<b>LeAdQA-34B</b>	<b>73.8 (+2.1)</b>	<b>79.4 (+1.7)</b>	<b>77.0 (+1.8)</b>

Table 2: VideoQA accuracy on NExT-GQA. LeAdQA-3B' and LeAdQA-7B' are developed based on Qwen-3B and Qwen-7B respectively.

As demonstrated in Tables 1, 2, 3 and 4, VideoQA models incorporating visual grounding consistently outperform baseline methods across all datasets. LeAdQA achieves SOTA VideoQA performance by treating temporal grounding as an auxiliary objective that supplements the primary QA task. While existing approaches like SeViLA and VideoTree demonstrate visual localization capabilities, their inability to model causal relationships constrains QA accuracy. LeAdQA addresses this through explicit causal reasoning, proving particularly effective for understanding dynamic processes and event progression. Our results demonstrate that causal reasoning effectively compensates for

grounding inaccuracies by providing essential contextual relationships, confirming that visual grounding and temporal alignment are complementary for effective video reasoning.

Model	Tem.	Cau.	Des.	Avg.
InternVideo (Wang et al. 2022b)	43.4	48.0	65.1	49.1
SeViLA (Yu et al. 2024)	61.3	61.5	75.6	63.6
MVU (Ranasinghe et al. 2024)	55.4	48.1	64.1	55.2
LLoVi (Zhang et al. 2023)	61.0	69.5	75.6	63.6
VideoAgent (Wang et al. 2025)	64.5	72.7	81.1	71.3
MoReVQA (Min et al. 2024)	56.1	52.7	71.8	60.2
IG-VLM (Kim et al. 2024)	63.6	69.8	74.7	68.6
LangRepo-7B (Kahatapitiya et al. 2024)	45.7	57.8	61.9	54.6
LangRepo-12B (Kahatapitiya et al. 2024)	51.4	64.4	69.1	60.9
LVNet (Park et al. 2024)	65.5	75.0	81.5	72.9
VideoTree (Wang et al. 2024c)	67.0	75.2	81.3	73.5
Tarsier-7B (Wang et al. 2024a)	66.4	71.7	81.9	71.6
<b>LeAdQA-7B</b>	66.6	72.5	82.3	72.1
	(+0.2)	(+0.8)	(+0.6)	(+0.5)
Tarsier-34B (Wang et al. 2024a)	<u>74.4</u>	<u>80.5</u>	<u>85.3</u>	<u>79.3</u>
<b>LeAdQA-34B</b>	<b>75.7</b>	<b>81.9</b>	<b>86.6</b>	<b>80.6</b>
	<b>(+1.3)</b>	<b>(+1.4)</b>	<b>(+1.3)</b>	<b>(+1.3)</b>

Table 3: VideoQA accuracy on NExT-QA.

Model	CW	CH	Tem.	Avg.
SeViLA (Yu et al. 2024)	-	-	-	60.9
LLoVi (Zhang et al. 2023)	68.4	67.4	51.1	64.0
IG-VLM (Kim et al. 2024)	-	-	-	64.2
LangRepo-7B (Kahatapitiya et al. 2024)	56.9	60.2	42.1	53.8
LangRepo-12B (Kahatapitiya et al. 2024)	62.8	62.4	47.8	59.1
LVNet (Park et al. 2024)	75.0	74.4	62.1	71.7
Tarsier-7B	69.9	69.9	59.6	67.4
<b>LeAdQA-7B</b>	<b>71.2</b>	<b>70.2</b>	<b>60.0</b>	<b>68.2</b>
	(+1.3)	(+0.3)	(+0.4)	(+0.8)
Tarsier-34B	<u>79.4</u>	<u>78.8</u>	<u>69.9</u>	<u>76.9</u>
<b>LeAdQA-34B</b>	<b>80.4</b>	<b>83.0</b>	<b>70.9</b>	<b>78.5</b>
	(+1.0)	(+4.2)	(+1.0)	(+1.6)

Table 4: VideoQA accuracy on IntentQA.

Table 2 demonstrates that our method can utilize various MLLMs as backbones and consistently improve their performance, highlighting the versatility of LeAdQA across different model architectures. The results in Table 3 show that multimodal models extend video understanding capabilities through enhanced semantic alignment and scalability, achieving substantial improvements over LLoVi’s caption-based approach. This performance advantage stems from superior cross-modal alignment that overcomes inherent single-modality limitations, particularly in complex rea-

soning tasks requiring temporal and causal understanding. Table 4 reveals consistent performance gains across all question types, with particularly notable improvements in CW (Causal How) questions. This pronounced effect indicates that LLM-based causal reasoning effectively complements visual evidence by reconstructing event chains that conventional approaches typically miss. Notably, the Tarsier-34B model shows greater performance improvements, suggesting that model scale and visual grounding operate synergistically to enhance video comprehension.

## Ablation Study

**Impact of QA Pair Rewriting with GPT-4.** Table 5 demonstrates that GPT-based causal rewriting consistently enhances performance under uniform grounding conditions, with the "+Causal Rewriting" variant achieving superior results across all question categories. The most substantial improvement appears in causal questions (Cau.), validating GPT’s proficiency in identifying and modeling causal relationships. Notably, concurrent improvements in temporal and descriptive questions indicate that semantic restructuring strengthens visual-textual alignment beyond the scope of causal reasoning alone.

Setting	Tem.	Cau.	Des.	Avg.
<i>Varying Grounding (w/ Causal Rewriting)</i>				
Random Sampling	72.0	79.9	84.3	78.0
Uniform Sampling	74.4	80.5	85.3	79.3
Ground-Truth Segments	79.5	82.6	85.3	82.1
<i>Varying Rewriting (w/ Uniform Grounding)</i>				
w/o Causal Rewriting	74.4	80.5	85.3	79.3
<b>+ Causal Rewriting (ours)</b>	<b>75.7</b>	<b>81.9</b>	<b>86.8</b>	<b>80.6</b>

Table 5: Ablation study on temporal grounding and causal rewriting on NEX-T-QA.

**Impact of Video Temporal Grounding.** We systematically examine how temporal grounding precision influences answer accuracy on the NEX-T-QA dataset using Tarsier-34B, maintaining uniform experimental conditions throughout. As illustrated in Table 5, we evaluate three sampling strategies: (1) random frame sampling, (2) uniform keyframe sampling, and (3) ground-truth segment sampling. Our analysis reveals a strong positive correlation between grounding precision and QA performance. The results establish that temporal coherence is fundamental to effective video comprehension, with structured sampling methods significantly outperforming random frame selection. Furthermore, precise visual grounding enhances reasoning quality by directing model attention to relevant visual content, while explicit causal modeling substantially improves understanding of event dynamics, especially in causal reasoning scenarios. These findings collectively underscore that effective video question answering demands the seamless integration of temporal structure, accurate visual localization, and comprehensive causal relationship modeling.

## In-depth Analysis

**Parameter Analysis for Interval Fusion.** Table 6 presents our evaluation of the interval fusion strategy on the NEX-T-QA validation set using Tarsier-34B with uniform 16-frame sampling. We investigate how the number of top-k candidate intervals and the IoU threshold for merging influence overall performance. Our analysis uncovers a critical trade-off in temporal fusion parameters: while increasing K initially improves answer quality by capturing additional visual cues, raising the IoU threshold degrades performance, indicating that overlapping intervals introduce noise that disrupts the reasoning process. An IoU threshold of 0.3 achieves optimal balance, effectively filtering irrelevant temporal segments while preserving essential events.

Top-K	IoU threshold				
	0.1	0.3	0.5	0.7	0.9
<b>Top-1</b>	<b>79.0</b>	78.9	78.9	78.8	78.6
<b>Top-3</b>	<b>79.5</b>	<b>79.5</b>	79.3	79.2	78.3
<b>Top-5</b>	<b>80.2</b>	<b>80.2</b>	79.4	79.4	73.3

Table 6: Impact of Top-K candidate intervals and IoU thresholds on Accuracy performance in NEX-T-QA with Tarsier-34B (16 frames).

**Frame Sampling Strategy for Answer Generation.** We systematically compare three sampling strategies: random, uniform, and our proposed query-focused sampling within grounded intervals. The results presented in Figure 3. Our findings demonstrate that random sampling consistently underperforms uniform sampling across all configurations, though temporal sorting narrows this performance gap, reinforcing the significance of temporal coherence. Notably, Figure 3 shows that query-focused sampling achieves comparable accuracy to uniform sampling while using fewer frames (32 vs. 48 frames: 81.2% vs. 81.2%), confirming our framework’s ability to eliminate irrelevant frames with minimal computational overhead. Furthermore, our experiments reveal distinct optimal frame requirements across model scales: Tarsier-7B reaches peak performance with 8 frames, showing diminishing returns beyond this threshold due to computational constraints, while Tarsier-34B continues improving up to 48 frames while maintaining processing efficiency.

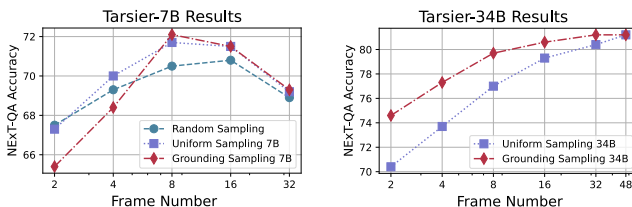


Figure 3: Tarsier-7B (left) and Tarsier-34B (right): VideoQA Accuracy vs. Frame Count.

## Conclusion

We present LeAdQA, an efficient framework designed to enhance multimodal reasoning in MLLMs for VideoQA through causal-aware question refinement and context-aware temporal grounding. By reformulating question-option pairs to address causal gaps, LeAdQA facilitates precise grounding of relevant visual content, thereby improving answer accuracy while reducing computational overhead. Experimental results demonstrate consistent improvements in modeling causal relationships and contextual understanding across various video reasoning tasks. Future research will focus on extending this framework to longer videos by exploring hierarchical comprehension and frame token compression techniques for more accurate understanding.

## References

- Achiam, J.; Adler, S.; Agarwal, S.; Ahmad, L.; Akkaya, I.; Aleman, F. L.; Almeida, D.; Altenschmidt, J.; Altman, S.; Anadkat, S.; et al. 2023. Gpt-4 technical report. *arXiv preprint arXiv:2303.08774*.
- Alayrac, J.-B.; Donahue, J.; Luc, P.; Miech, A.; Barr, I.; Hasson, Y.; Lenc, K.; Mensch, A.; Millican, K.; Reynolds, M.; et al. 2022. Flamingo: a visual language model for few-shot learning. *Advances in neural information processing systems*, 35: 23716–23736.
- Bai, S.; Chen, K.; Liu, X.; Wang, J.; Ge, W.; Song, S.; Dang, K.; Wang, P.; Wang, S.; Tang, J.; Zhong, H.; Zhu, Y.; Yang, M.; Li, Z.; Wan, J.; Wang, P.; Ding, W.; Fu, Z.; Xu, Y.; Ye, J.; Zhang, X.; Xie, T.; Cheng, Z.; Zhang, H.; Yang, Z.; Xu, H.; and Lin, J. 2025. Qwen2.5-VL Technical Report. *arXiv preprint arXiv:2502.13923*.
- Chu, W.; Xue, H.; Zhao, Z.; Cai, D.; and Yao, C. 2018. The forgettable-watcher model for video question answering. *Neurocomputing*, 314: 386–393.
- Fei, H.; Wu, S.; Ji, W.; Zhang, H.; Zhang, M.; Lee, M.-L.; and Hsu, W. 2024. Video-of-thought: Step-by-step video reasoning from perception to cognition. In *Forty-first International Conference on Machine Learning*.
- Fu, T.-J.; Li, L.; Gan, Z.; Lin, K.; Wang, W. Y.; Wang, L.; and Liu, Z. 2023. An empirical study of end-to-end video-language transformers with masked visual modeling. In *Proceedings of the IEEE/CVF Conference on Computer Vision and Pattern Recognition*, 22898–22909.
- Gao, J.; Sun, C.; Yang, Z.; and Nevatia, R. 2017. Tall: Temporal activity localization via language query. In *Proceedings of the IEEE international conference on computer vision*, 5267–5275.
- Guo, Y.; Liu, J.; Li, M.; Liu, Q.; Chen, X.; and Tang, X. 2024. Trace: Temporal grounding video llm via causal event modeling. *arXiv preprint arXiv:2410.05643*.
- Islam, M. M.; Ho, N.; Yang, X.; Nagarajan, T.; Torresani, L.; and Bertasius, G. 2024. Video ReCap: Recursive Captioning of Hour-Long Videos. In *Proceedings of the IEEE/CVF Conference on Computer Vision and Pattern Recognition*, 18198–18208.
- Kahatapitiya, K.; Ranasinghe, K.; Park, J.; and Ryoo, M. S. 2024. Language repository for long video understanding. *arXiv preprint arXiv:2403.14622*.
- Kim, W.; Choi, C.; Lee, W.; and Rhee, W. 2024. An image grid can be worth a video: Zero-shot video question answering using a vlm. *arXiv preprint arXiv:2403.18406*.
- Lei, J.; Berg, T. L.; and Bansal, M. 2021. Detecting moments and highlights in videos via natural language queries. *Advances in Neural Information Processing Systems*, 34: 11846–11858.
- Lei, J.; Yu, L.; Bansal, M.; and Berg, T. L. 2018. Tvqa: Localized, compositional video question answering. *arXiv preprint arXiv:1809.01696*.
- Li, J.; Li, D.; Savarese, S.; and Hoi, S. 2023a. BLIP-2: Bootstrapping Language-Image Pre-training with Frozen Image Encoders and Large Language Models. *arXiv:2301.12597*.
- Li, J.; Wei, P.; Han, W.; and Fan, L. 2023b. Intentqa: Context-aware video intent reasoning. In *Proceedings of the IEEE/CVF International Conference on Computer Vision*, 11963–11974.
- Li, Y.; Wang, X.; Xiao, J.; Ji, W.; and Chua, T.-S. 2022. Invariant grounding for video question answering. In *Proceedings of the IEEE/CVF Conference on Computer Vision and Pattern Recognition*, 2928–2937.
- Lin, K. Q.; Zhang, P.; Chen, J.; Pramanick, S.; Gao, D.; Wang, A. J.; Yan, R.; and Shou, M. Z. 2023. Univtq: Towards unified video-language temporal grounding. In *Proceedings of the IEEE/CVF International Conference on Computer Vision*, 2794–2804.
- Liu, H.; Li, C.; Wu, Q.; and Lee, Y. J. 2024. Visual instruction tuning. *Advances in neural information processing systems*, 36.
- Lu, J.; Yang, J.; Batra, D.; and Parikh, D. 2016. Hierarchical question-image co-attention for visual question answering. *Advances in neural information processing systems*, 29.
- Maaz, M.; Rasheed, H.; Khan, S.; and Khan, F. S. 2023. Video-chatgpt: Towards detailed video understanding via large vision and language models. *arXiv preprint arXiv:2306.05424*.
- Min, J.; Buch, S.; Nagrani, A.; Cho, M.; and Schmid, C. 2024. Morevqa: Exploring modular reasoning models for video question answering. In *Proceedings of the IEEE/CVF Conference on Computer Vision and Pattern Recognition*, 13235–13245.
- Moon, W.; Hyun, S.; Park, S.; Park, D.; and Heo, J.-P. 2023. Query-dependent video representation for moment retrieval and highlight detection. In *Proceedings of the IEEE/CVF conference on computer vision and pattern recognition*, 23023–23033.
- Park, J.; Ranasinghe, K.; Kahatapitiya, K.; Ryoo, W.; Kim, D.; and Ryoo, M. S. 2024. Too Many Frames, not all Useful: Efficient Strategies for Long-Form Video QA. *arXiv preprint arXiv:2406.09396*.
- Radford, A.; Kim, J. W.; Hallacy, C.; Ramesh, A.; Goh, G.; Agarwal, S.; Sastry, G.; Askell, A.; Mishkin, P.; Clark, J.;

- et al. 2021. Learning transferable visual models from natural language supervision. In *International conference on machine learning*, 8748–8763. PMLR.
- Ranasinghe, K.; Li, X.; Kahatapitiya, K.; and Ryoo, M. S. 2024. Understanding Long Videos in One Multimodal Language Model Pass. *arXiv preprint arXiv:2403.16998*.
- Ren, S.; He, K.; Girshick, R.; and Sun, J. 2016. Faster R-CNN: Towards real-time object detection with region proposal networks. *IEEE transactions on pattern analysis and machine intelligence*, 39(6): 1137–1149.
- Seo, A.; Kang, G.-C.; Park, J.; and Zhang, B.-T. 2021. Attend what you need: Motion-appearance synergistic networks for video question answering. *arXiv preprint arXiv:2106.10446*.
- Tan, R.; Sun, X.; Hu, P.; Wang, J.-h.; Deilamsalehy, H.; Plummer, B. A.; Russell, B.; and Saenko, K. 2024. Koala: Key frame-conditioned long video-LLM. In *Proceedings of the IEEE/CVF Conference on Computer Vision and Pattern Recognition*, 13581–13591.
- Tran, D.; Bourdev, L.; Fergus, R.; Torresani, L.; and Paluri, M. 2015. Learning spatiotemporal features with 3d convolutional networks. In *Proceedings of the IEEE international conference on computer vision*, 4489–4497.
- Wang, J.; Yuan, L.; Zhang, Y.; and Sun, H. 2024a. Tarsier: Recipes for training and evaluating large video description models. URL <https://arxiv.org/abs/2407.00634>, 8.
- Wang, P.; Yang, A.; Men, R.; Lin, J.; Bai, S.; Li, Z.; Ma, J.; Zhou, C.; Zhou, J.; and Yang, H. 2022a. Ofa: Unifying architectures, tasks, and modalities through a simple sequence-to-sequence learning framework. In *International conference on machine learning*, 23318–23340. PMLR.
- Wang, X.; Si, Q.; Wu, J.; Zhu, S.; Cao, L.; and Nie, L. 2024b. ReTaKe: Reducing Temporal and Knowledge Redundancy for Long Video Understanding. *arXiv preprint arXiv:2412.20504*.
- Wang, X.; Zhang, Y.; Zohar, O.; and Yeung-Levy, S. 2025. Videoagent: Long-form video understanding with large language model as agent. In *European Conference on Computer Vision*, 58–76. Springer.
- Wang, Y.; Li, K.; Li, Y.; He, Y.; Huang, B.; Zhao, Z.; Zhang, H.; Xu, J.; Liu, Y.; Wang, Z.; et al. 2022b. Internvideo: General video foundation models via generative and discriminative learning. *arXiv preprint arXiv:2212.03191*.
- Wang, Z.; Yu, S.; Stengel-Eskin, E.; Yoon, J.; Cheng, F.; Bertasius, G.; and Bansal, M. 2024c. VideoTree: Adaptive Tree-based Video Representation for LLM Reasoning on Long Videos. *arXiv preprint arXiv:2405.19209*.
- Wei, Y.; Liu, Y.; Yan, H.; Li, G.; and Lin, L. 2023. Visual causal scene refinement for video question answering. In *Proceedings of the 31st ACM International Conference on Multimedia*, 377–386.
- Wu, Y.; Hu, X.; Sun, Y.; Zhou, Y.; Zhu, W.; Rao, F.; Schiele, B.; and Yang, X. 2025. Number it: Temporal grounding videos like flipping manga. In *Proceedings of the Computer Vision and Pattern Recognition Conference*, 13754–13765.
- Xiao, J.; Shang, X.; Yao, A.; and Chua, T.-S. 2021. Nextqa: Next phase of question-answering to explaining temporal actions. In *Proceedings of the IEEE/CVF conference on computer vision and pattern recognition*, 9777–9786.
- Xiao, J.; Yao, A.; Li, Y.; and Chua, T.-S. 2024. Can i trust your answer? visually grounded video question answering. In *Proceedings of the IEEE/CVF Conference on Computer Vision and Pattern Recognition*, 13204–13214.
- Xu, H.; He, K.; Sigal, L.; Sclaroff, S.; and Saenko, K. 2018. Text-to-clip video retrieval with early fusion and re-captioning. *arXiv preprint arXiv:1804.05113*, 2(6): 7.
- Xu, Y.; Wei, Y.; Zhong, S.; Chen, X.; Qi, J.; and Wu, B. 2024. Exploring Question Guidance and Answer Calibration for Visually Grounded Video Question Answering. In *Findings of the Association for Computational Linguistics: EMNLP 2024*, 3121–3133.
- Yang, A.; Miech, A.; Sivic, J.; Laptev, I.; and Schmid, C. 2022. Zero-shot video question answering via frozen bidirectional language models. *Advances in Neural Information Processing Systems*, 35: 124–141.
- Yu, S.; Cho, J.; Yadav, P.; and Bansal, M. 2024. Self-chained image-language model for video localization and question answering. *Advances in Neural Information Processing Systems*, 36.
- Yu, T.; Yu, J.; Yu, Z.; Huang, Q.; and Tian, Q. 2020. Long-term video question answering via multimodal hierarchical memory attentive networks. *IEEE Transactions on Circuits and Systems for Video Technology*, 31(3): 931–944.
- Zang, C.; Wang, H.; Pei, M.; and Liang, W. 2023. Discovering the real association: Multimodal causal reasoning in video question answering. In *Proceedings of the IEEE/CVF Conference on Computer Vision and Pattern Recognition*, 19027–19036.
- Zhang, C.; Lu, T.; Islam, M. M.; Wang, Z.; Yu, S.; Bansal, M.; and Bertasius, G. 2023. A simple llm framework for long-range video question-answering. *arXiv preprint arXiv:2312.17235*.
- Zhao, Y.; Misra, I.; Krähenbühl, P.; and Girdhar, R. 2023. Learning video representations from large language models. In *Proceedings of the IEEE/CVF Conference on Computer Vision and Pattern Recognition*, 6586–6597.